Journal of Bio- and Tribo-Corrosion (2019) 5:3
https://doi.org/10.1007/s40735-018-0194-4

Tribocorrosion of Porous Titanium Used in Biomedical Applications

Arjun Manoj[1] · Ashish K. Kasar[1] · Pradeep L. Menezes[1]

Received: 31 July 2018 / Revised: 9 October 2018 / Accepted: 20 October 2018 / Published online: 30 October 2018

Abstract
Titanium and its alloys have become increasingly important in the dental and orthopedic fields due to its good machinability, high yield strength, good ductility, excellent corrosion resistance, and superior biocompatibility compared to other materials. However, an inherent drawback of using pure titanium and its alloys as implant material is the significant mismatch between the moduli of bone and titanium, resulting in the stress shielding effect, fibrous tissue ingrowth, and bone resorption, and therefore reducing the lifespan of the implant. Porous titanium is thus a suitable candidate as implant material due to its ability to be manufactured to a specific Young's modulus—typically that of bone. Porous titanium has the unique advantage of allowing bone tissue ingrowth into the open space of the implants, thereby accelerating the osseointegration process. The human body as well as the oral cavity is a highly complex environment in which the simultaneous interaction between wear and corrosion, namely tribocorrosion, takes place. Thus, understanding these interactions is of great interest in order to characterize the degradation mechanisms of porous titanium materials used as implants. This paper reviews the state-of-the-art of porous titanium as a viable biomedical implant material. A significant part of this paper is focused on how porous titanium is manufactured and how its parameters are controlled. The following sections focus on the corrosion, wear, and tribocorrosion aspects of porous titanium implant materials. Finally, this review also determines the current limitations in the field and provides future directions in this field.

Keywords Implant · Porous titanium · Corrosion · Wear · Tribocorrosion

1 Introduction

In recent years, titanium and its alloys have become increasingly important and widely used in the dental and orthopedic fields due to its high yield strength, good ductility, excellent corrosion resistance, and superior biocompatibility compared to other materials [1–3]. Musculoskeletal disorders are one of the most significant health problems facing the world today, with an estimated cost $254 billion to society each year, and has been increasing over the past decade [4, 5]. Due to improvements in surgical techniques and the development in more intelligent assistive technologies, there has been a significant increase in the demand for prostheses, orthopedic implants, and dental implants. Examples of hip and knee biomedical implants are shown in Fig. 1. Over the past few decades, dental implants have come to be a significant part of rehabilitation in oral cavity due to tooth loss or disease. Further, it has been predicted that over one million implants will be used per year [6]. In the field of dentistry, survival rates of dental implants exceeded 94% in the first 10 years, indicating their relative success [7]. However, it has been seen that every fifth dental implant placed develops peri-implantitis in the initial stages of placement [1, 4–6]. The proportion of peri-implant mucositis ranged from 19 to 65% and peri-implantitis ranged from 1 to 47%, respectively [8, 9]. This shows that there is significant risk of acquiring these conditions, especially earlier in the implantation stage. Figure 2 shows the various causes of failure for biomedical implants and when a replacement or revision surgery is needed. The two most important aspects to consider when choosing implant materials are the relative biocompatibility and its corrosion resistance in the body. Titanium has been a promising material for biological implants due to its superior biocompatibility and high corrosion resistance in the body. A major issue facing the use of titanium implants, however, is the significant difference between the Young's modulus of titanium (110 GPa) and bone (10–30 GPa) [5–7].

✉ Pradeep L. Menezes
pmenezes@unr.edu

[1] Department of Mechanical Engineering, University of Nevada Reno, Reno, NV 89557, USA

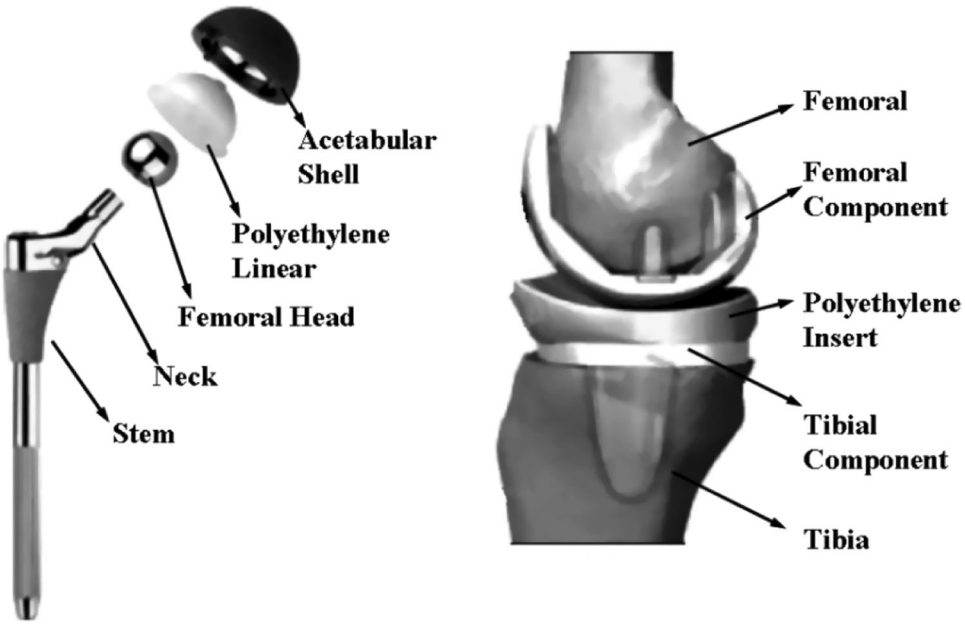

Fig. 1 Total hip and knee replacement implants [11]

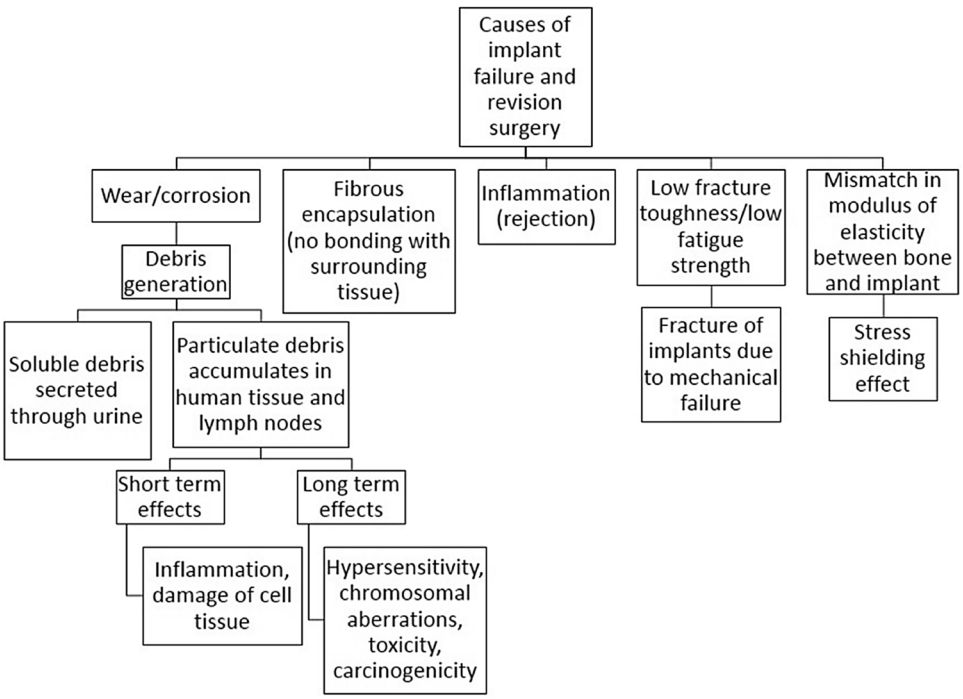

Fig. 2 Causes for revision or replacement surgery due to implant failure, adapted from Geetha et al. [11]

This difference in modulus leads to an inefficient transfer of load between the implant and supporting bone, which is typically known as the stress shielding effect. This phenomenon causes bone resorption, or loss of bone density of the supporting bone due to inadequate loading, which can lead to higher rates of bone fracture and implant failure [10].

It has been hypothesized that the application of implant materials with porous microstructures can significantly reduce the stress shielding effect, improve overall bone implant osseointegration by allowing bone ingrowth, and is currently an active area of research [3, 12, 13]. Though there is research devoted to development special titanium alloys with lower moduli, a porous microstructure allows the possibility of bone tissue ingrowth within the structure along with the transport of essential body fluids, which makes it an attractive alternative [1, 2, 14, 15]. Titanium is highly biocompatible; however, it cannot form a direct bond with surrounding bone to allow for new bone formation which

helps the fixation of the implant to the bone. If the implant fails to fixate to the surrounding bone, implant failure can occur in the early stages, and this is particularly common for patient groups with diseases like chronic inflammation, diabetes, and osteoporosis among many others [16, 17].

The human body is a highly dynamic environment where conditions are never constant. This means that whatever implant material is used is required to be highly stable against these dynamic conditions. Between the bone and implant, there is relative cyclic motion causing wear and wear debris to be formed. Additionally, these materials and structures are surrounded by corrosive body fluids, leading way to a wear–corrosion synergism interaction [18, 19]. This synergistic interaction between tribology and corrosion, or tribocorrosion, causes deterioration of surfaces of the materials involved. It is known that these simultaneous actions of both wear and corrosion cause a significantly higher total material loss as compared to the interaction of each individual mechanism without the other [20].

There exists various surface modification and coating technologies which can be utilized to improve the properties of implant materials. One such technique that is actively studied is the anodic surface treatment, which can lead to better wear, corrosion, and tribocorrosion resistance, and the formation of a porous microstructure on the surface of the material. This results in a better biological interaction between the implant and surrounding structure due to the controllability of the surface topography and porosity [20–22]. Another method by which these materials can be modified is by using powder metallurgy to manipulate the concentration of porosities and will be further discussed in this paper.

As of 2018, there are many studies on the mechanical behavior of porous titanium; however, studies on the wear and corrosion behavior separately are relatively unknown. Furthermore, studies on the synergism between wear and corrosion of porous titanium and titanium alloys are limited. In this review paper, wear, corrosion, and tribocorrosion behaviors of porous titanium and titanium alloys used for biomedical applications are discussed. An attempt is made to describe the commonly used methods by which these materials are manufactured and how the processing and material parameters are accurately controlled. Additionally, some specific applications of porous implants within the body and the specific interaction between the body and the implant material are discussed.

2 Materials

In the field of orthopedic and dental implants, the amount of materials that can be utilized are highly limited. The implant must have superior biocompatibility properties, high strength and fatigue resistance, phenomenal corrosion resistance, and longevity in the human body. Thus, only very specific metals and alloys are used. This includes 316L stainless steel (316L SS) [23–25], titanium and its alloys [23, 26, 27], cobalt-based (Co–Cr) alloys [23, 28, 29], magnesium alloys with surface coatings [30–32], and tantalum [23, 33, 34]. Table 1 shows the commonly used materials approved by the United States Food and Drugs Administration for use as biomedical implants and their primary applications.

These materials are commonly utilized for their excellent biocompatibility and corrosion resistance properties, as well as their ability to reduce the stress shielding effect due to their comparable modulus to bone. However, these materials have a modulus in the range from approximately 86–220 GPa [23–29], and so there is still a significant mechanical mismatch between implant material and surrounding bone. This problem gives rise to the use and implementation of porous materials or materials with various surface modifications, which can allow interlocking between the implant and surrounding bone. With the use of a 3-dimensional open-pore structure within the implant, tissue ingrowth can be supported and has seen success in various animal testing [35]. It is possible to accurately control the mechanical properties of the implants by closely monitoring and controlling the pore parameters, such as pore volume,

Table 1 Commonly used implant materials and their applications as biomedical implants

Materials	Applications	References
Stainless steels	Orthopaedic implants, dental implants, orthodontic wires, screws, plates, hip nails, rovascular implants, monobloc hip stems	[23–25]
Co-based alloys	Orthodontic wire leads, femoral stems, bearing surface implant, load-bearing implants, bone implant applications, total joint replacements, total hip implants, removable partial dentures, vascular stents	[23, 26, 27]
Ti-based alloys	Dental implants, orthodontic wire leads, total hip replacements, heart valve parts, vascular stents, bone substitution implants, skeletal prostheses	[23, 28, 29]
Mg alloys with surface coatings	Biodegradable orthopedic implants	[30–32]
Ta-based alloys	Wire structures for plastic and neurosurgery	[23, 33, 34]

density, interconnectedness, and pore size. This can allow the stress shielding effect to be reduced by allowing transfer of stress from the implant to the bone, while also providing space for bone attachment and proliferation into the implant allowing for transfer of body fluids [35]. The common types of fabrication methods employed in manufacturing porous materials and implants are discussed in Sect. 3.

The selection of metals in biological systems is significant due to the human being a highly complex environment. Metals in the biological systems may experience ion release, corrosion, and wear over prolonged use. Thus, the biocompatibility of these materials, as defined by their carcinogenicity and toxicity, must be considered to decrease the rate of failure [36]. Over the past few decades, titanium and its alloys have become a gold industrial standard from which orthopedic and dental implants are manufactured. It is well known that aluminum and vanadium may cause biological issues such as scar tissue formation and sterile abscess; however, materials such as titanium, zirconium, tantalum, and niobium show excellent biocompatibility [36]. Furthermore, recent studies show that β-stabilizing elements can further improve its biocompatibility while providing an overall lower elastic modulus. These β-type titanium alloys consist of elements mentioned above such as zirconium, tantalum, molybdenum, and niobium. A few such examples of these alloys include Ti13Nb13Zr [37], which was found to have a modulus of 79 GPa, Ti29Nb13Ta4.6Zr [38], and Ti35Nb5Ta7Zr [39], both of which were found to have moduli in the range of 55–65 GPa. Even though these new β-alloys have excellent biocompatibility and better moduli compared to that of bone, the modulus is still approximately double that of bone, indicating that there is still risk of poor osseointegration and bone resorption. Further, these solid titanium materials still do not allow for the possibilities of bone tissue ingrowth [40]. However, porous versions of these β-alloys have potential as biomedical implants. Liu et al. [41] prepared porous a β-type Ti24Nb4Zr8Sn using electron beam melting and was able to achieve moduli around 0.95 GPa with 75% porosity. Thus, porous β-alloys can be a potential candidate for biomedical implants and is currently an active area of study.

When developing new porous materials, especially ones that will become load-bearing, an important consideration to make is how the mechanical strength and fatigue properties are changed [42]. This gives rise to development of techniques that can both address and manipulate these parameters to obtain the desired characteristics for a biomedical application. There have been some prior studies to create structures that can match the modulus of cortical bone; however, these studies did not consider the relationship between processing parameters and the effect of porosity on the mechanical properties [4, 43]. Presently, several methods are used to produce porous titanium. They are listed as follows: powder sintering, hollow powder sintering, pore formation via gas expansion or addition of solid space holder, sintering of powders on scaffold, reactive sintering/densification of powders in the presence of gas, entrapped gas techniques, and additive manufacturing methods such as electron beam melting. When employed, these techniques allow for processing of porous titanium materials, and based on their application, porous structures with varying pore shape, size, and distribution can be obtained. Figure 3 shows many of these processing methods and how the porous structure is formed.

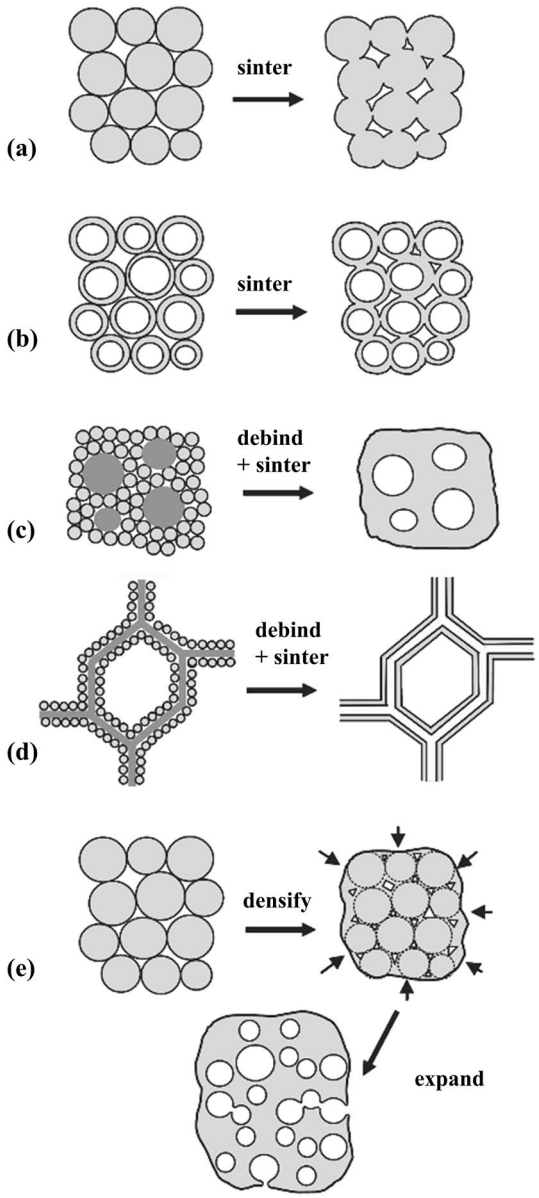

Fig. 3 Development of porous structure using—**a** powder sintering, **b** hollow powder sintering, **c** secondary pore formation via gas expansion methods or by space holder technique, **d** powder sintering using fugitive scaffold, **e** expansion of trapped gas bubbles [44]

3 Processing Methods

3.1 Powder Sintering Methods

Powder sintering is the simplest of methods by which porous materials can be manufactured. The equipment requirement is minimal, and the processes typically only have one or two steps. A major drawback of this method is that the pore size and volume are dependent on powder size, shape, and the compaction pressure applied.

3.1.1 Uniform Powder Sintering

The simplest technique by which porous titanium can be processed is based on partial sintering of titanium powders. Cirincione et al. [45] sintered loose Ti–6Al–4V powders at 1000 °C from 0.5 to 24 h, where porosities ranging from 41 and 55% were achieved. The highest compressive strength of 55 MPa was found in samples containing 49% porosity, and the strength of the samples was attributed to the formation of necks between powder particles. Uniaxial pressing can be employed to accelerate the kinetics of densification of unalloyed titanium samples. Schuch et al. [46] and Taylor et al. [47] investigated the behavior of hot pressing titanium powder above and below its allotropic temperature of approximately 882 °C, which resulted in a porosity ranging between 5 and 35%. Oh et al. [48, 49] achieved 5–37% porosity in spherical unalloyed titanium powders that were sintered with and without applied pressure. It was observed that compressive yield strength and Young's modulus decreased linearly with increasing porosity. The stiffness of the porous titanium samples was found to be nearly that of human bone (20 GPa) at around 30% porosity. In another study, Oh et al. [50] achieved a gradient in porosity in unalloyed titanium powders by using layer of titanium powders with varying particle sizes, which were sintered both with and without applied stress. Ricceri and Matteazzi et al. [51] used cold isostatic pressing and sintering of Ti–6Al–4V powder to obtain samples with 26% porosity. Furthermore, they eliminated the closed pores without affecting the open pores using containerless hot isostatic pressing. Spark plasma sintering is another method by with sintering time can be decreased [52]. Porosities of 30% were achieved using this method at temperatures ranging from 560 to 700 °C and the sintering times ranged from 3 to 20 min. The mechanical properties of the spark plasma sintered samples were further improved by annealing at 1000 °C. Porosities ranging from 35 and 60% were reported by Thieme et al. [53] for sintered titanium powders. The bending strengths of these samples were found to be between 5 and 190 MPa and Young's modulus from 5 to 80 GPa. It was demonstrated that adding 1.5 wt% silicon to the titanium powders accelerated the sintering of coarse powder with no measurable effects on the bulk strength of the titanium foams after processing. Further, graded porous titanium samples were produced by stacking various powder layers with differences in particle size and silicon content. The pore volume fraction varied from 22 to 45% and the pore size varied from 48 to 200 µm.

One of the main limitations of the powder sintering method is that the pore size and shape are limited to the available titanium powder size and shape. A maximum porosity of 50% was found for spherical powders with pores being highly non-spherical. To overcome the problem of low pore fraction, one of the solutions is to use titanium wires. Murray and Semple [54] demonstrated that a crimpled 130 µm diameter wire sintered around 1600 °C resulted in a titanium foam with an open-cell structure with porosity from 45 to 50%. A higher pore volume could have been achieved using this method simply by reducing the sintering temperature. The porosity is a result of the inner space of the powders as well as the space between powders due to partial sintering. Sypeck et al. [55] used this method to sinter 0.5–1.4 mm diameter hollow Ti–6Al–4V spheres for 24 h, resulting in a foam with 73% porosity. However, a low compressive strength of 6.2 MPa and weak bonding was observed between the spheres due to their inherently large size.

3.1.2 Non-uniform Powder Sintering with Gaseous Blowing Agent

Another method by which porous materials can be processed is via a gaseous blowing agent. Using this method, large, secondary pores are created using a gas within a preform of titanium powders containing small, primary pores. The primary pores are a result of the actual spacing between each titanium particle. The primary pores are eliminated upon sintering of the samples, and the secondary pores remain unchanged (shown in Fig. 3c). One of the main advantages of this method is that volume fraction and shape of the pores can be controlled regardless of the characteristics of the titanium powder. However, the secondary pores are much larger when compared to the titanium powders, and as a result, contamination from the binder and titanium powders results in residual primary pores due to incomplete sintering. Furthermore, uniaxial pressing cannot be used because it would result in collapse of the secondary pores, and as a result, the mechanical properties are typically much weaker than pressed samples. Jee et al. [56] was able to obtain metallic titanium foams with 90–95% porosity using a CO_2-based blowing agent to create secondary pores; however, the subsequent sintering was only partially successful because of

the ash residues from the resin. Hurysz et al. [57] combined the hollow-sphere and gas-blowing processes and obtained hollow titanium spheres. Upon thermal treatment and sintering, a density over 96% was achieved for the titanium powders in the sphere walls. The spheres had a diameter ranging from 1 to 6 mm and a wall thickness of 0.1 mm.

3.1.3 Non-uniform Powder Sintering Using Solid Space Holder

Other commonly used method by which large secondary pores can be introduced into a titanium powder preform is to use a space holder. The pore forming agents offer unique properties such as high and low melting points, water-solubility, low-cost, and non-toxicity, making them easily removable during the sintering-dissolution process. When manufacturing porous titanium samples using a space holder technique, pure or alloyed titanium powders are combined in a mixing process with NaCl, ammonium hydrogen carbonate, or another polymetric material for a certain amount of time [42]. The powder and space holder mixture is then pressed and thus has enough strength to prevent collapse when the space holder is removed and sintered. Aşık and Bor [58] used the space holder technique with spherical magnesium powders mixed with Ti–6Al–4V powders. The magnesium space was then vaporized, and subsequent sintering resulted in samples with porosities ranging from 51 to 65%. As magnesium has a much lower melting point than titanium, it vaporizes without reacting with the titanium powders. In a similar study, Wheeler et al. [59] created porous Ti and Ti–6Al–4V samples by using magnesium powder as space holder. The space holder was evaporated at 1000 °C, and the samples were sintered at 1400 °C. The resulting samples had porosity ranging from 25 to 82%, Young's moduli and yield strengths ranging from 3 to 9 GPa and 15 to 607 MPa, respectively. Kostornov et al. [60, 61] sintered a mixture of titanium powder with copper and a wax space holder, stearin. This combination produced a transient liquid phase during sintering and produced foams with porosity from 25 to 70%. In a similar study, Bram et al. [62] used urea as a space holder in making titanium foams. The urea was removed at 200 °C, and subsequent sintering at 1400 °C resulted in porosity ranging from 60 to 77% and pore size from 0.1 to 2.4 mm. The pore size was dependent on the urea particle size. A yield stress of 10 and 100 MPa was observed for the samples with 77 and 60% porosity, respectively. Wen et al. [12] obtained a porosity of 78% in titanium samples using ammonium hydrogen carbonate as space holder. The space holder was decomposed at 200 °C, and the resulting titanium was sintered at 1200 °C for 2 h. The resulting foam was found to have a Young's modulus of 5.3 GPa and compressive strength of 35 MPa. These moduli and compressive strength were found to be close to that of human cancellous bone, which ranges from 10 to 40 GPa and 3 to 20 MPa, respectively. Rausch et al. [63] obtained titanium foams ranging from 55 to 80% porosity using polymer granules as space holder. The space holder was chemically removed at 130 °C and subsequently sintered at 1100–1250 °C. The foams had a Young's modulus ranging from 0.3 to 16 GPa and a tensile strength from 1.5 to 30 MPa. Zhao et al. [64] fabricated NiTi alloys having a porosity of approximately 90% using NaCl particles as space holder. It was observed that porosity increased linearly with increasing volume percentage of NaCl particles under the same temperature and time conditions. Jakubowicz et al. [65] studied porous titanium structures in the range from 50 to 70% porosity using spherical and polyhedral-shaped $C_{12}H_{22}O_{11}$. Their findings showed that spherical-shaped space holder particles mixed with 100 mesh Ti powders showed improved sintering when compared to polyhedral-shaped space holder particles mixed with 325 mesh Ti powders. Andersen et al. [66] coated Styrofoam spheres with titanium powder and binder. The polymer was removed by heat treatment, and the spheres were then sintered. The resulting hollow titanium spheres had a diameter of 4 mm and 0.125 mm wall thickness. This method, however, results in contamination of the titanium during processing, so it is not typically used to create any type of foams.

3.1.4 Powder Sintering Using Fugitive Scaffold

In the previous technique mentioned above [66], a polymer scaffold, which acts as a fugitive space holder, is repeatedly coated with titanium powder and binder. Upon removal of the scaffold and binder, and subsequent sintering, an open-cell structure with hollow titanium struts is produced. This method was first demonstrated by Kupp et al. [67]. Application of this method results in three types of pores: primary porosity within the struts due to initial powder particle size, secondary porosity as a result of the previously occupied scaffold, and open tertiary porosity between the struts. A porosity 88% was obtained by Li et al. [68] using this process with Ti–6Al–4V powders and polyurethane elastomeric scaffold foams. The resulting foams had a compressive strength of 10 MPa. It was later observed that a second application of powder slurry following the initial sintering and re-sintering with the second layer resulted in increased compressive strength of 36 MPa and density of 80%, due to removal of flaws from the titanium struts [69].

3.2 Gas Expansion Processing Methods

The sintering processes mentioned above do not allow for easy control of pore characteristics such as pore

connectivity, size, and volume. These parameters are predetermined by the original primary and secondary pores in the powder preform. In gas expansion processing methods, superplastic expansion and creep result in pore parameters being independent of the original powder size and shape. As a result, however, this processing method is more complex and requires more specialized equipment, and the resulting foams rarely have a pore volume fraction exceeding 50%.

3.2.1 Creep and Superplastic Expansion Processes

Porous titanium processing using solid-state expansion of pressurized pores was first explored by Kearns and Blenkinsop [70]. It is a process in which powders are packed into a canister that is subsequently evacuated and then filled with argon gas. Hot isostatic pressing is then used to densify the powders; since argon does not react with titanium, it is entrapped in the titanium matrix in the form of high-pressure, micron-sized argon bubbles. Upon cooling and removal of the canister, the titanium billet undergoes a heat treatment process. Expansion of the gases is possible due to the reduced strength of the titanium matrix upon heat treatment. It was observed that increasing the foaming temperature or back fill pressure of the argon allowed controllability of the porosity within the foam due to the reduction in creep strength of matrix. A porosity of 30% was achieved at a temperature of 1240 °C and 0.1 atm backfill pressure. Furthermore, it was found that hot-working the titanium billets before heat treatment resulted in elongation of the pores, leading to anisotropic expansion upon heat treatment. Dunand and Teisen and Davis et al. [71, 72] used a similar process on commercially pure titanium powders and obtained a porosity of 22–26%. A Young's modulus of 60 GPa and yield stress of 200 MPa were observed for these samples.

The creep expansion process has relatively slow kinetics due to low deformation rates exhibited by titanium, and the resulting foam does not have a high volume of porosity due to merging of pores with each other, leading to escape of the foaming gas. Induced superplasticity, however, allows for faster foaming rates and higher tensile ductilities. Duand and Teisen [71] were the first to manufacture commercially pure Ti and Ti–6Al–4V powders using transformation superplasticity, which was achieved by thermally cycling the material powders around its allotropic transformation temperatures. Davis et al. [72] applied a uniaxial stress during the titanium foaming process. Though this did not have any effects on the overall porosity, the pores were elongated in the direction of the applied stress. A porosity of 41% was achieved with a Young's modulus of 39 GPa and a yield stress of approximately 120 MPa.

3.3 Additive Manufacturing Method using Electron Beam Melting

Additive manufacturing methods have significantly become more affordable in recent decades and have become an exciting area of study for the fabrication of porous titanium materials for biomedical applications. In the additive manufacturing process, complex parts and shapes are manufactured using computer aided design in a layer-by-layer process. Porous metals with a predefined internal and external architecture can be fabricated.

Electron beam melting (EBM) is a manufacturing process by which metal powders can be melted in a layer-by-layer fashion with an electron beam. Metallurgical bonding between each of the resulting layers makes it possible to fabricate a complete part. The EBM process requires a vacuum chamber in order to ensure the beam has a resistance-free path so that the metal powders do not react with the atmosphere. The electron beam is generated using a tungsten filament, such as in a typical scanning electron microscope. Upon exciting the electrons in the filament, two magnetic fields organize the electron beam in the proper shape and direction and metal melting takes place. The metal particles are fused together due to the transfer of kinetic energy from the electrons into thermal energy. Parthasarathy et al. [73] fabricated Ti–6Al–4V samples with porosities ranging from approximately 50–70%, with pore sizes from 765 to 1960 µm, respectively. Further, the compressive stress of these samples varied from 7.28 to 163.02 GPa for the 50 and 70% porosities, respectively; shown in Fig. 4 are the resulting stress–strain curves. The samples were found to have a Young's modulus from 0.57 to 2.92 GPa and a compressive strength of 7.3 to 163 MPa. Heinl et al. [74] was able to use electron beam melting method to fabricate

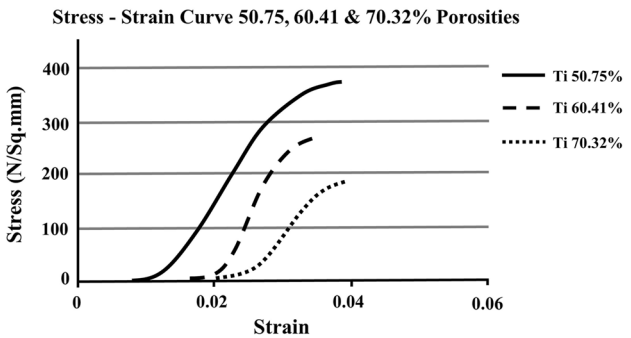

Fig. 4 Stress–strain curves for the porous titanium samples with 50.75%, 60.41%, and 70.32% porosity values [73]

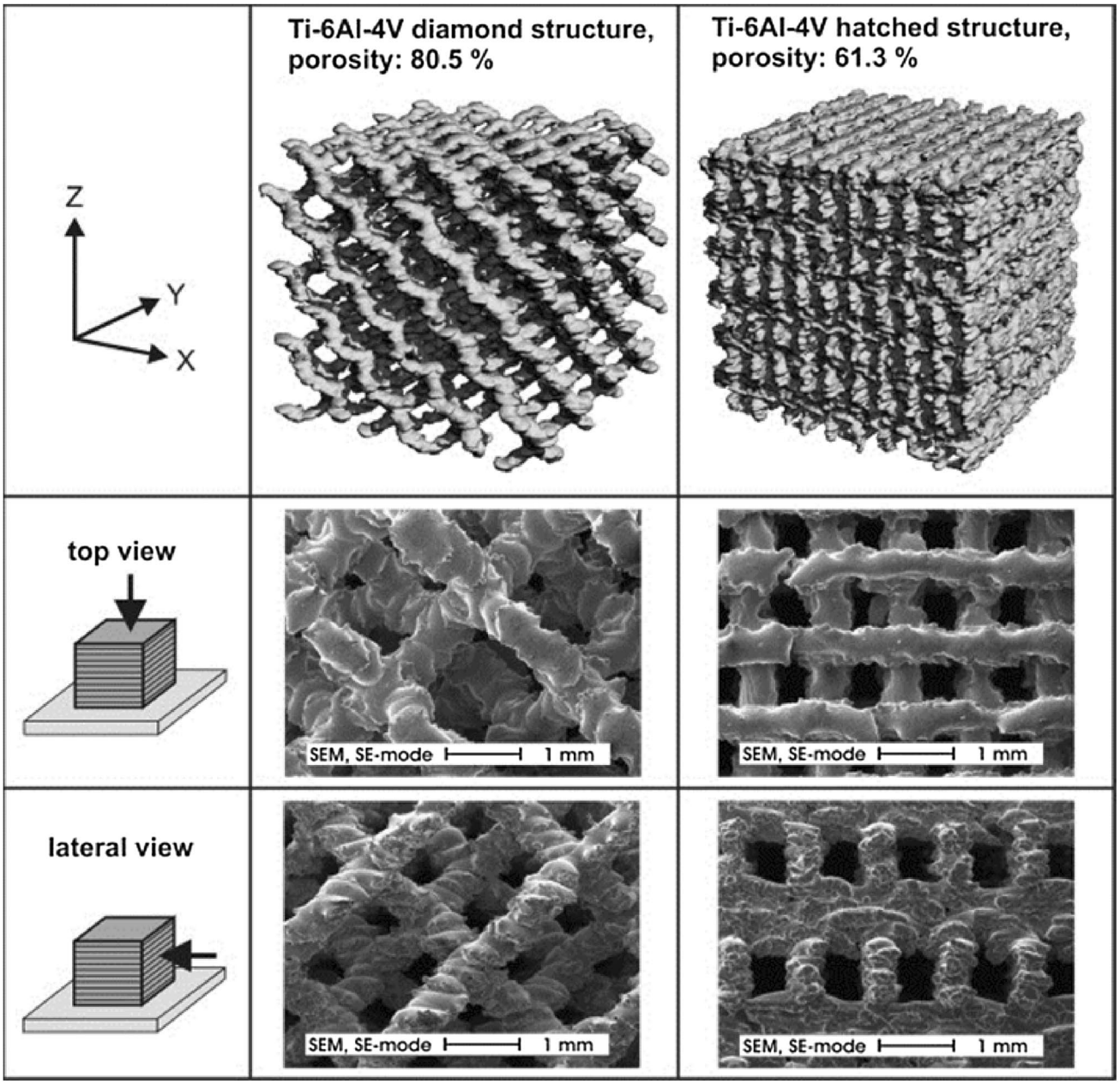

Fig. 5 Ti–6Al–4V diamond and hatched geometries produced using EBM and their resulting SEM micrographs [74]

porous Ti–6Al–4V structures with varying geometries, which yielded porosities of 80.5% for the diamond shape, and porosities of 61.3% for the hatched shape. Figure 5 shows each of the two geometries that were fabricated, along with its SEM micrographs. These results show that elastic behavior of these materials can be manipulated according to patient needs. Further, these implants could be custom-made for each patient.

4 Degradation Processes

4.1 Corrosion of Porous Titanium Materials

Corrosion is the result of an electrochemical change due to the simultaneous oxidation and reduction that results in metallic oxides, hydroxides, or sulfides. This

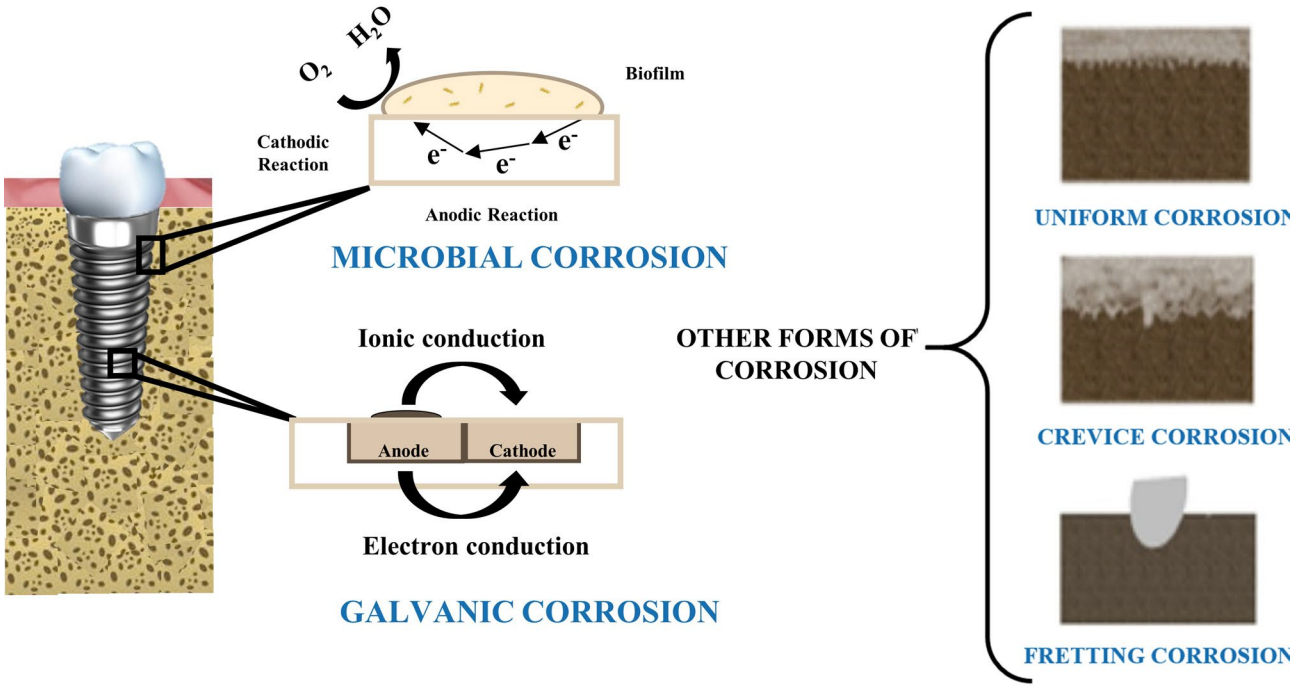

Fig. 6 Possible types of corrosion in dental implants [75]

is typically an undesirable trait; however, materials like aluminum and titanium form a protective oxide layer or passive layer that can be advantageous because of the electrochemical change. Shown in Fig. 6 are the types of corrosion that a typical dental implant is subject to [75]. Titanium is known for its highly unreactive passive layer forming characteristics. In air or an aqueous environment, titanium forms a stable oxide layer that ranges from 1 to 5 nm in thickness. This is an excellent characteristic that allows titanium to perform better than almost all other biocompatible materials when used as an implant material. However, despite these excellent corrosion resistance properties of solid titanium, porous materials behave differently when implemented in these environments. Seah et al. [76] studied the passivation behavior of solid titanium and porous titanium. It was observed that pore morphology, whether isolated or interconnected, plays a significant role in the overall performance of the material. Furthermore, the authors found that higher compaction pressure on the green pellets prior to sintering played a large role in determining the overall pore density along with electrochemical potential. A 623 mV drop in potential as the compaction pressure was varied from 5 to 18 tons was observed, resulting from pores being interconnected in the low-pressure case and isolated in the high-pressure case. The authors suggested that electrolyte species were being trapped in the isolated pores, resulting in a lack of oxygen supply, and thus poor maintenance of the titanium oxide layer. In the case of interconnected pores, however, it was suggested that the free flow of electrolyte within the structure allowed replacement of oxygen, thereby allowing passive layer formation. Fojt et al. [77] observed similar behavior in Ti39Nb alloy processed using a similar method, with porosities ranging from 0 to 33%, finding that samples of up to 15% porosity exhibited corrosion behavior akin to that of dense samples. Samples with pore densities higher than 15% exhibited localized corrosion behavior. Furthermore, repassivation of the samples did

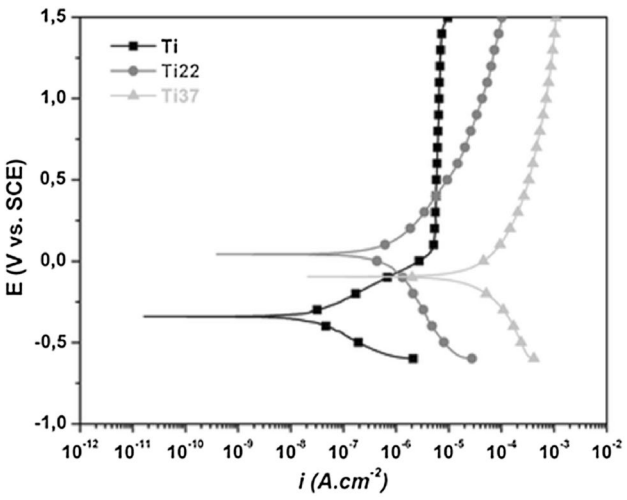

Fig. 7 Potentiodynamic polarization curves of titanium with varying levels of porosity [78]

not occur at 33% porosity, but did for the samples at 24% porosity, indicating a higher corrosion process. Similarly, Alves et al. [78] studied the corrosion behavior of titanium having 30 and 50% nominal porosity. Potentiodynamic polarization and electrochemical impedance spectroscopy revealed a less stable oxide layer in samples with increased porosity, which was attributed to the interconnectivity and complexity of the pores, resulting in a less protective oxide layer and higher corrosion current values. Figure 7 shows the potentiodynamic polarization curves of pure titanium, titanium with 22 and 37% porosity. There lacks a well-defined passive region in the porous samples as compared to the dense sample. This can likely be attributed to the inconsistencies of the oxide film formed in the inner surfaces of the innermost pores due to heterogeneities in the overall structure. A higher current density was observed on the porous samples likely due to improper or incomplete penetration of the electrolyte through the inner pores of the samples.

Li et al. [79] investigated the implant potential of NiTi shape memory alloy (SMA) and found that pore density and pore morphology played a significant role in the corrosion process. The researchers observed a breakdown of the oxide layer and pitting at low anodic potentials in the porous samples. As in previous studies mentioned above, the corrosion properties of solid NiTi were superior to those of porous samples. However, Stergioudi et al. [6] observed increased corrosion resistance in NiTi samples with 18% porosity from 7% porosity contrary to previous research works. It was found that increase in compaction pressure, and thus lower porosity, increased the corrosion current density. This variation from previous works was associated with the pore morphology of the 7% porous NiTi. Microstructure observations revealed that pores are sharper, smaller, and closer together in the 7% porous sample, thereby promoting exhaustion of oxygen supply by trapping of electrolyte species. Furthermore, it was observed that pore morphology changes to smoother and wider pores that allowed the free flow of electrolyte species, thus promoting oxide film formation.

4.2 Wear of Porous Titanium Materials

The human body has been found to have remarkable tribological characteristics. The intrinsic properties of articular cartilage combined with synovial fluid create highly optimized lubrication conditions for bones and joints [80]. As people age, however, these properties are degraded, leading to a degeneration of bones, joints, and surrounding fluids. When the natural joint can no longer perform adequately, surgical intervention may be necessary to alleviate pain and discomfort [80]. When considering implant materials, their degradation over time must be considered to ensure that the materials in use do not fail before the intended time. One important aspect to consider, and especially when determining the feasibility of porous implant materials, is their wear and tribological properties under varying loading and boundary conditions.

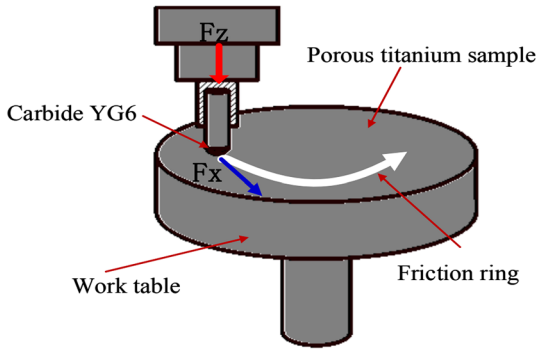

Fig. 8 Pin-on-disk tester used by Liu et al. [83]

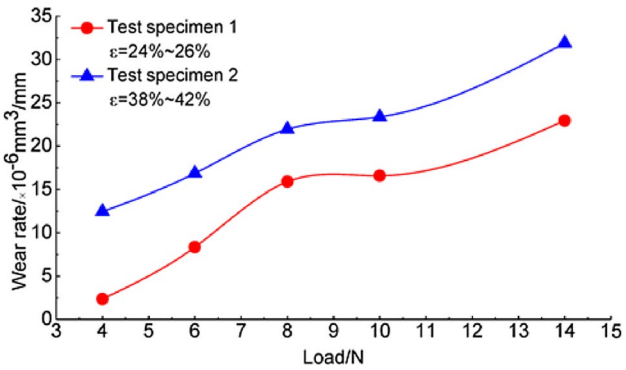

Fig. 9 Wear rates of pure titanium with 24–26 and 38–42% porosity [83]

Wu et al. [81] studied the wear behavior of 18 and 36 vol% porous NiTi samples. The wear test experiments revealed that the sample with 36 vol% porosity exhibited a higher wear resistance than the 18 vol% sample. Similarly, the coefficient of friction of the 36 vol% sample was also found to be lower than the 18 vol% sample. Wear scar analysis revealed that these surprising results were due to wear debris filling in the pores and providing a mechanism by which the counter-body could roll over the surface. Similarly, Salahinejad et al. [82] found that AISI 316L stainless steel exhibited similar behavior in the wear mechanisms of porous samples as compared to dense samples.

Liu et al. [83] studied the friction and wear properties of pure porous titanium using tungsten carbide as the counter material. Though this study was focused on metal machining applications, the observed results of the behavior of titanium can be applied toward biomedical implants. The authors investigated two sets of titanium samples using the

sintering method with 24 and 38% porosity. A pin-on-disk tester, shown in Fig. 8, was used to do the tribological testing under different loading conditions. The results of the wear and friction tests are shown in Fig. 9. On comparing the specimens of different porosity, it was observed that the wear rate decreased as the porosity increased, resulting in a reduction of the wear resistance of the material. It is known that as the porosity of a material increases, its modulus and other mechanical properties are typically reduced. Further, an increase in the overall porosity of the materials leads to an increase in the fracture phenomenon and thus a higher accumulation of wear debris. The wear mechanisms of porous titanium at room temperature were attributed to abrasive and slight oxidative wear.

Prabu et al. [84] made a steel-titanium alloy with densities of 85, 90, and 95% using powder sintering methods. These samples thus had porosities of 15, 10, and 5%, respectively, as the density increased. A pin-on-disk tester at varying loading conditions was used to determine the wear behavior of each of the samples. During wear testing, the samples with $< 10\%$ porosity were found to have its pores filled with wear debris, thereby enhancing wear resistance and increasing the real contact area. The opposite behavior was observed in samples with $> 10\%$ porosity. The mass loss increased as the porosity and load increased due to thermal softening of the material and delamination wear at higher loads. From these limited studies that does not consider biological conditions, but simply similar materials, porosity has a significant influence on the wear rates of titanium materials. From these results, it can be inferred that more testing in required in the wear of porous titanium materials to have a thorough model to optimize material porosities based on the loading conditions that the implants will be subjected to.

4.3 Tribocorrosion of Porous Titanium Materials

To date, studies related to the wear–corrosion synergism, or tribocorrosion, of porous titanium materials are severely limited. These investigations have been limited to a few research groups, and it is only recently that the wear–corrosion synergism of porous materials have gained traction. Toptan et al. [1] has given one of the first insights of the tribocorrosion behavior of highly porous titanium. The researchers produced the samples via powder metallurgy using the

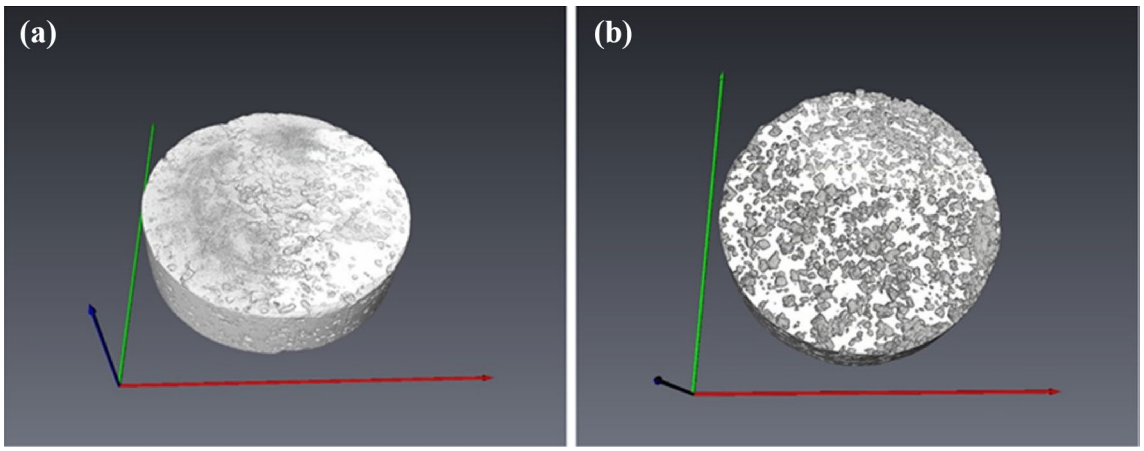

Fig. 10 Microtomographic reconstructions of titanium samples at **a** 22% porosity and **b** 37 porosity [1]

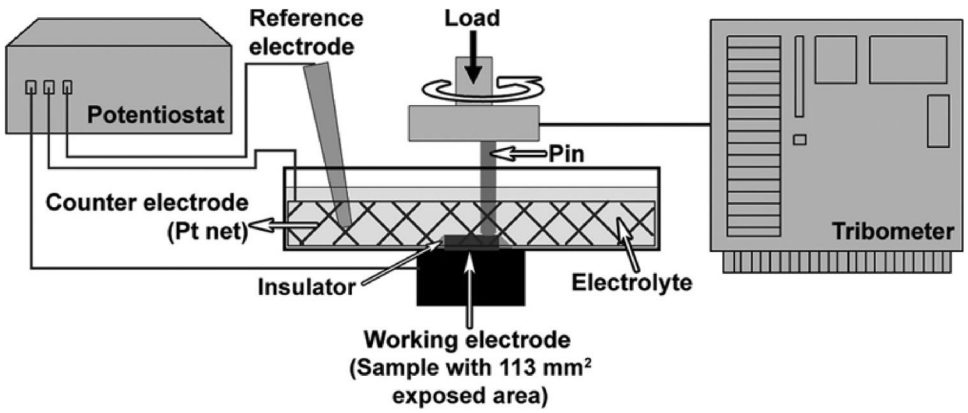

Fig. 11 Tribocorrosion test setup [1]

space holder technique with urea as the space holder. 30 and 50 vol% urea were blended with grade 2 titanium powders and pressed uniaxially at 350 MPa. The resulting pellets were then heated to 450 °C to evaporate the space holder followed by sintered at 1100 °C under vacuum for 3 h. The titanium samples were found to have a porosity of 22 and 37% using three-dimensional microtomographic reconstructions, as shown in Fig. 10. The samples were then anodically treated with β-glycerophosphate disodium salt pentahydrate and calcium acetate monohydrate at room temperature to bio-functionalize the samples. Following this, the samples were placed into a tribocorrosion test cell to perform tribocorrosion experiments, as shown in Fig. 11. Before testing, the samples were etched and placed in a desiccator for 24 h.

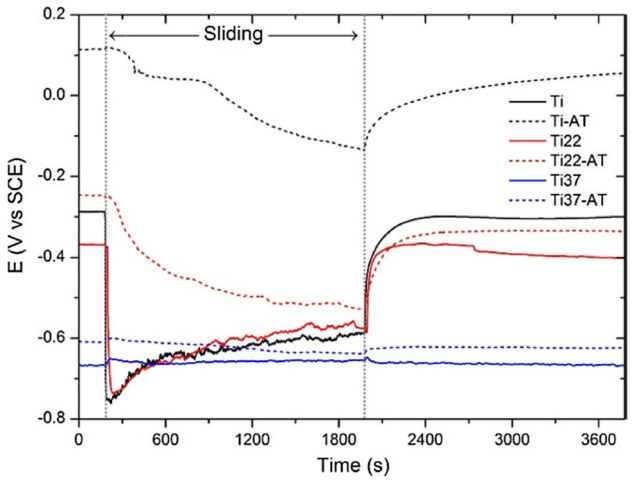

Fig. 12 Open circuit potential before, during, and after sliding on dense, porous, and biofunctionalized titanium samples [1]

The electrolyte used for all the tests was a 9 g/L solution of NaCl to simulate a biological environment.

It was found that the dense titanium samples exhibited higher wear than porous samples. As expected, however, the anodically treated samples always performed better, regardless of the porosity. Furthermore, the oxide layers on the dense and porous samples were thought to play a protective and lubricative role in the wear experiments. Oxide layer debris was found in the pores and likely reduced the overall wear and third-body wear. After the wear experiments, open circuit potential (OCP) testing was conducted in conjunction to the wear tests. Figure 12 shows the OCP curves for dense titanium (Ti), anodically treated dense titanium (Ti-AT), 22% porosity titanium (Ti22), anodically treated 22% porosity titanium (Ti22-AT), 37% porosity titanium (Ti37), and anodically treated 37% porosity titanium (Ti37-AT). It was observed that the OCP values of both the 22% and 37% volume porosity samples displayed more negative corrosion potentials, indicating a higher tendency for corrosion. It was determined that differences in the formation of oxide layers on the pore surfaces prevented the formation of a proper passive layer on the porous samples. Additionally, the counter material generally slid over the anodized surfaces, thus resulting in reduced damage on the anodized surfaces. Once sliding started, there was an immediate decrease in OCP for all the samples. This was due to the sudden destruction of the passive or oxide layer. After sliding, however, all the samples were again able to achieve the initial OCP values, showing that all the samples, regardless of porosity, were able to repassivate properly. In the 37% volume porosity samples, however, it was observed that the OCP values remained stable throughout sliding. This behavior was attributed to the accumulation of oxide debris in the pores itself,

Table 2 Tribocorrosion studies of various dense titanium alloys

Titanium alloy	Tribological test	Electrochemical test	Solution	References
Ti6Al4V	Reciprocating, ball-on-plate, unidirectional	OCP, applied potential	NaCl, Artificial saliva, artificial saliva + fluorides, artificial + pH variation	[85, 87, 88]
Ti-G2, Ti-G5, Ti6Al4V, Ti6Al4V ELI	Unidirectional, ball-on-plate	Applied potential	Phosphate buffered solution	[89]
Ti29Nb13Ta4.6Zr	Reciprocating, ball-on-disk	OCP, applied potential	Hank's balance salt solution	[90]
Cp Ti, Ti6Al4V	Ball-on-disk	OCP, applied potential	Artificial saliva, artificial saliva + lipopolysaccharide	[86, 91]
Cp Ti	Reciprocating, ball-on-plate	OCP	Modified Fusayama, modified Fusayama + fluorides	[92]
Ti6Al4V ELI, Ti13Nb13Zr	Block-on-disk	–	Simulated body fluid	[93]
Ti35Nb7.2Zr5.7Ta, Ti35Nb7.2Zr5.7Ta0.5b, Ti13Nb13Zr0.5B, Ti13Nb13Zr	Pin-on-disk	–	Hank's, bovine serum	[94–96]
Ti6Al4V	Reciprocating, ball-on-plate	OCP, applied potential, potential sweep	Simulated body fluid	[97]

reducing the overall third-body wear, which itself can damage the oxide film.

Additional tribocorrosion studies have been done on titanium and titanium alloys by Licausi et al. [85] and Matthew et al. [86]; however, these studies have been limited to dense materials and not porous samples. Table 2 shows further studies that have been performed on dense titanium materials. However, these tests have not been conducted on porous samples of the same material. From these studies, it can be observed that the reciprocating and unidirectional ball-on-plate and ball-on-disk are the most common methods by which the tribological aspects of these materials are characterized. Simultaneity, the commonly used electrochemical methods are open circuit potential and applied potential testing in various electrolytes that simulate the biological environment. These studies, however, do not simulate actual physical conditions that are present in the human body as they are all either one-dimensional or two-dimensional loading conditions. In fact, biological implants are subjected to three-dimensional loading conditions as well as impact loading conditions, and these studies do not consider these aspects. The lack of studies and literature on the tribocorrosion of porous titanium material suggest that more research needs to be performed on the synergistic effect between wear and corrosion of implant materials in the human body.

5 Future Directions

Current research suggests that there is a severe gap in the current knowledge regarding the degradation mechanisms of porous titanium and titanium alloys, especially in a biological environment. The exact relationship between volume and size of porosities in relation to the wear mechanism is not exactly known. Similarly, contradictory results in corrosion testing of these types of materials show that there is still disagreement in current practices. Additionally, corrosion and tribocorrosion tests need to be performed with more varying levels of porosity to determine exactly how the pores influence corrosion properties as well as oxide layer formation. Furthermore, potentiostatic and potentiodynamic tests need to be conducted in conjunction with wear tests to better simulate the bone/implant interface. Based on the present understanding of the tribocorrosion mechanisms of porous titanium materials as biomedical implants, we suggest the following research directions:

- The relationship between pore volume and tribocorrosion parameters for different titanium alloys needs to be investigated that can help to optimize the pore parameters based on the alloys.
- Comprehensive testing of porous materials as implant materials that incorporate mechanical (friction, wear, lubrication, fatigue), chemical (corrosion, pH), and biological (protein, bacteria, disease) parameters are required to gain a full understanding of how these materials perform while in the human body.
- More extensive electrochemical tests during tribotesting such as potentiodynamic and potentiostatic polarization need to be carried out to predict the corrosion rate. Corrosion and wear rate prediction will be advantageous to compute the life of implants.
- Additionally, there is a need for theoretical models upon which porous titanium structures could be manufactured for a given Young's modulus, yield strength, and other bio-functionalization methods.

6 Conclusions

Porous titanium material has been beneficial compared to dense titanium due to its ability for allowing bone tissue ingrowth, thereby improving osseointegration. Furthermore, porous titanium has a lower Young's modulus that matches with the modulus of natural bone leading to decreased stress shielding. The manufacturing process of porous titanium plays a deciding role for corrosion and wear properties because the porous structure contains more passive materials generated by tribolayer formation. Therefore, using the suitable process to achieve desired porosity size and density will lower the degradation by tribocorrosion. However, increase in porosity up to a certain limit has shown good mechanical and corrosion properties based on the materials. Beyond this limit, materials have shown lower strength due to neck formation between particles and lower corrosion resistance due to repassivation. Porous biomaterials have been shown to have beneficial applications as implants and implant materials. Their superior biocompatibility, corrosion resistance, and high strength make them an attractive option in the medical field. Studies have shown that approximately 6% of dental implants fail and around 20% of new implants are used to replace failed implants. Though small, this failure rate suggests that there needs to be better and more accurate methods by which these degradation mechanisms can be characterized and manipulated.

References

1. Toptan F, Alves A, Pinto A, Ponthiaux P (2017) Tribocorrosion behavior of bio-functionalized highly porous titanium. J Mech Behav Biomed Mater 69:144–152
2. Guo Y, Georgarakis K, Yokoyama Y, Yavari A (2013) On the mechanical properties of TiNb based alloys. J Alloys Compd 571:25–30
3. Chen X-B, Li Y-C, Du Plessis J, Hodgson PD, Wen C (2009) Influence of calcium ion deposition on apatite-inducing ability

of porous titanium for biomedical applications. Acta Biomater 5(5):1808–1820
4. Krishna BV, Bose S, Bandyopadhyay A (2007) Low stiffness porous Ti structures for load-bearing implants. Acta Biomater 3(6):997–1006
5. Fretwurst T, Nelson K, Tarnow D, Wang H-L, Giannobile W (2018) Is metal particle release associated with peri-implant bone destruction? An emerging concept. J Dent Res 97(3):259–265
6. Stergioudi F, Vogiatzis C, Pavlidou E, Skolianos S, Michailidis N (2016) Corrosion resistance of porous NiTi biomedical alloy in simulated body fluids. Smart Mater Struct 25(9):095024
7. Menini R, Dion M-J, So SK, Gauthier M, Lefebvre L-P (2006) Surface and corrosion electrochemical characterization of titanium foams for implant applications. J Electrochem Soc 153(1):B13–B21
8. Derks J, Tomasi C (2015) Peri-implant health and disease. A systematic review of current epidemiology. J Clin Periodontol 42:S158–S171
9. Schwarz F, Derks J, Monje A, Wang HL (2018) Peri-implantitis. J Clin Periodontol 45:S246–S266
10. Huiskes R, Weinans H, Van Rietbergen B (1992) The relationship between stress shielding and bone resorption around total hip stems and the effects of flexible materials. Clin Orthopaed Relat Res 274:124–134
11. Geetha M, Singh AK, Asokamani R, Gogia AK (2009) Ti based biomaterials, the ultimate choice for orthopaedic implants—a review. Prog Mater Sci 54(3):397–425
12. Wen C, Mabuchi M, Yamada Y, Shimojima K, Chino Y, Asahina T (2001) Processing of biocompatible porous Ti and Mg. Scripta Mater 45(10):1147–1153
13. Wen C, Yamada Y, Shimojima K, Chino Y, Hosokawa H, Mabuchi M (2002) Novel titanium foam for bone tissue engineering. J Mater Res 17(10):2633–2639
14. Martins JRS Jr, Grandini CR (2014) The influence of heat treatment on the structure and microstructure of Ti-15Mo-xNb system alloys for biomedical applications. Materials Science Forum. https://doi.org/10.4028/www.scientific.net/MSF.783-786.1255
15. Correa DRN, Kuroda PAB, Grandini CR (2014) Structure, microstructure, and selected mechanical properties of Ti-Zr-Mo alloys for biomedical applications. Adv Mater Res 992:75–80
16. Gosavi S, Gosavi S, Alla R (2013) Titanium: a miracle metal in dentistry. Trends Biomater Artif Organs 27(1):42–46
17. Hu X, Shen H, Shuai K, Zhang E, Bai Y, Cheng Y, Xiong X, Wang S, Fang J, Wei S (2011) Surface bioactivity modification of titanium by CO_2 plasma treatment and induction of hydroxyapatite: in vitro and in vivo studies. Appl Surf Sci 257(6):1813–1823
18. Landolt D, Mischler S, Stemp M, Barril S (2004) Third body effects and material fluxes in tribocorrosion systems involving a sliding contact. Wear 256(5):517–524
19. Marino CE, Mascaro LH (2004) EIS characterization of a Ti-dental implant in artificial saliva media: dissolution process of the oxide barrier. J Electroanal Chem 568:115–120
20. Teixeira M, Alves A, Silva FS, Pinto A, Toptan F (2015) Microstructural characterization of biofunctionalized titanium foams. Microsc Microanal 21(S5):55–56
21. Alves A, Oliveira F, Wenger F, Ponthiaux P, Celis J-P, Rocha L (2013) Tribocorrosion behaviour of anodic treated titanium surfaces intended for dental implants. J Phys D 46(40):404001
22. Fan X, Feng B, Weng J, Wang J, Lu X (2011) Processing and properties of porous titanium with high porosity coated by bioactive titania nanotubes. Mater Lett 65(19–20):2899–2901
23. Asri R, Harun W, Samykano M, Lah N, Ghani S, Tarlochan F, Raza M (2017) Corrosion and surface modification on biocompatible metals: a review. Mater Sci Eng C 77:1261–1274
24. Disegi J, Eschbach L (2000) Stainless steel in bone surgery. Injury 31:D2–D6
25. Hosseinalipour S, Ershad-Langroudi A, Hayati AN, Nabizade-Haghighi A (2010) Characterization of sol–gel coated 316L stainless steel for biomedical applications. Prog Org Coat 67(4):371–374
26. Calin M, Gebert A, Ghinea AC, Gostin PF, Abdi S, Mickel C, Eckert J (2013) Designing biocompatible Ti-based metallic glasses for implant applications. Mater Sci Eng C 33(2):875–883
27. Faeda RS, Tavares HS, Sartori R, Guastaldi AC, Marcantonio E Jr (2009) Evaluation of titanium implants with surface modification by laser beam: biomechanical study in rabbit tibias. Braz Oral Res 23(2):137–143
28. Liu J, Wang X, Wu B, Zhang T, Leng Y, Huang N (2013) Tribocorrosion behavior of DLC-coated CoCrMo alloy in simulated biological environment. Vacuum 92:39–43
29. Hedberg YS, Qian B, Shen Z, Virtanen S, Wallinder IO (2014) In vitro biocompatibility of CoCrMo dental alloys fabricated by selective laser melting. Dent Mater 30(5):525–534
30. Shadanbaz S, Dias GJ (2012) Calcium phosphate coatings on magnesium alloys for biomedical applications: a review. Acta Biomater 8(1):20–30
31. Dorozhkin SV (2014) Calcium orthophosphate coatings on magnesium and its biodegradable alloys. Acta Biomater 10(7):2919–2934
32. Jin W, Wang G, Lin Z, Feng H, Li W, Peng X, Qasim AM, Chu PK (2017) Corrosion resistance and cytocompatibility of tantalum-surface-functionalized biomedical ZK60 Mg alloy. Corros Sci 114:45–56
33. Gray J, Luan B (2002) Protective coatings on magnesium and its alloys—a critical review. J Alloys Compd 336(1–2):88–113
34. Hornberger H, Virtanen S, Boccaccini A (2012) Biomedical coatings on magnesium alloys—a review. Acta Biomater 8(7):2442–2455
35. Barrabés M, Sevilla P, Planell J, Gil F (2008) Mechanical properties of nickel–titanium foams for reconstructive orthopaedics. Mater Sci Eng C 28(1):23–27
36. Gepreel MA-H, Niinomi M (2013) Biocompatibility of Ti-alloys for long-term implantation. J Mech Behav Biomed Mater 20:407–415
37. Davidson J, Mishra A, Kovacs P, Poggie R (1994) New surface-hardened, low-modulus, corrosion-resistant Ti-13Nb-13Zr alloy for total hip arthroplasty. Bio-med Mater Eng 4(3):231–243
38. Kuroda D, Niinomi M, Morinaga M, Kato Y, Yashiro T (1998) Design and mechanical properties of new β type titanium alloys for implant materials. Mater Sci Eng A 243(1–2):244–249
39. Steinemann S, Winter G, Leray J (1980) Evaluation of biomaterials. Willey, New York, pp 5435–5438
40. Yavari SA, Ahmadi S, van der Stok J, Wauthlé R, Riemslag A, Janssen M, Schrooten J, Weinans H, Zadpoor AA (2014) Effects of bio-functionalizing surface treatments on the mechanical behavior of open porous titanium biomaterials. J Mech Behav Biomed Mater 36:109–119
41. Liu YJ, Li SJ, Wang HL, Hou WT, Hao YL, Yang R, Sercombe TB, Zhang LC (2016) Microstructure, defects and mechanical behavior of beta-type titanium porous structures manufactured by electron beam melting and selective laser melting. Acta Mater 113:56–67
42. Torres Y, Trueba P, Pavón J, Montealegre I, Rodríguez-Ortiz J (2014) Designing, processing and characterisation of titanium cylinders with graded porosity: an alternative to stress-shielding solutions. Mater Des 63:316–324
43. Traini T, Mangano C, Sammons R, Mangano F, Macchi A, Piattelli A (2008) Direct laser metal sintering as a new approach to fabrication of an isoelastic functionally graded material for manufacture of porous titanium dental implants. Dent Mater 24(11):1525–1533

44. Dunand DC (2004) Processing of titanium foams. Adv Eng Mater 6(6):369–376
45. Cirincione R, Anderson R, Zhou J, Mumm D, Soboyejo WO (2002) An investigation of the effects of sintering duration and powder sizes of the porosity and compression strength of porous Ti-6Al-4V. Processing and properties of lightweight cellular metals and structures. p 189
46. Schuh C, Noel P, Dunand D (2000) Enhanced densification of metal powders by transformation-mismatch plasticity. Acta Mater 48(8):1639–1653
47. Taylor N, Dunand D, Mortensen A (1993) Initial stage hot pressing of monosized Ti and 90% Ti-10% TiC powders. Acta Metall Mater 41(3):955–965
48. Oh I-H, Nomura N, Hanada S (2002) Microstructures and mechanical properties of porous titanium compacts prepared by powder sintering. Mater Trans 43(3):443–446
49. Oh I-H, Nomura N, Masahashi N, Hanada S (2003) Mechanical properties of porous titanium compacts prepared by powder sintering. Scripta Mater 49(12):1197–1202
50. Oh I-H, Segawa H, Nomura N, Hanada S (2003) Microstructures and mechanical properties of porosity-graded pure titanium compacts. Mater Trans 44(4):657–660
51. Riccent R, Matteazzi P (2001) Porous nanocrystalline Ti-alloy implants. Int J Powder Metall 37(4):61–66
52. Asaoka K, Kon M (2003) Sintered porous titanium and titanium alloys as advanced biomaterials. Mater Sci Forum 426:3079–3084
53. Thieme M, Wieters K-P, Bergner F, Scharnweber D, Worch H, Ndop J, Kim T, Grill W (2001) Titanium powder sintering for preparation of a porous functionally graded material destined for orthopaedic implants. J Mater Sci: Mater Med 12(3):225–231
54. Murray G, Semple JC (1981) Transfer of tensile loads from a prosthesis to bone using porous titanium. J Bone Joint Surg Br 63(1):138–141
55. Sypeck DJ, Parrish PA, Wadley HN (1998) Novel hollow powder porous structures. MRS Online Proc Libr Arch. https://doi.org/10.1557/PROC-521-205
56. Jee C, Guo Z, Evans J, Özgüven N (2000) Preparation of high porosity metal foams. Metall Mater Trans B 31(6):1345–1352
57. Hurysz K, Clark J, Nagel A, Hardwicke C, Lee K, Cochran J, Sanders T (1998) Steel and titanium hollow sphere foams. MRS Online Proc Libr Arch. https://doi.org/10.1557/PROC-521-191
58. Aşık EE, Bor Ş (2015) Fatigue behavior of Ti–6Al–4V foams processed by magnesium space holder technique. Mater Sci Eng A 621:157–165
59. Wheeler K, Karagianes M, Sump K (1983) Porous titanium alloy for prosthesis attachment. In: Titanium alloys in surgical implants. ASTM International, Phoenix
60. Kostornov A, Galstyan L, Mnatsakanyan S, Agayan S (1986) The physicomechanical properties of porous titanium base powder materials. Sov Powder Metall Met Ceram 25(11):909–911
61. Kostornov A, Agayan S (1990) Determining the quality of baking of porous titanium to porosity-free. Sov Powder Metall Met Ceram 29(10):804–807
62. Bram M, Stiller C, Buchkremer HP, Stöver D, Baur H (2000) High-porosity titanium, stainless steel, and superalloy parts. Adv Eng Mater 2(4):196–199
63. Rausch G, Banhart JE, Degischer H (2002) Handbook of cellular metals. Wiley, Weinheim
64. Zhao X, Sun H, Lan L, Huang J, Zhang H, Wang Y (2009) Pore structures of high-porosity NiTi alloys made from elemental powders with NaCl temporary space-holders. Mater Lett 63(28):2402–2404
65. Jakubowicz J, Adamek G, Pałka K, Andrzejewski D (2015) Micro-CT analysis and mechanical properties of Ti spherical and polyhedral void composites made with saccharose as a space holder material. Mater Charact 100:13–20
66. Andersen O, Waag U, Schneider L, Stephani G, Kieback B (2000) Novel metallic hollow sphere structures. Adv Eng Mater 2(4):192–195
67. Kupp D, Claar D, Flemmig K, Waag U, Goehler H (2002) Processing of controlled porosity titanium-based materials. Adv Powder Metall Part Mater (2):2–126
68. Li JP, Li SH, De Groot K, Layrolle P (2002)Preparation and characterization of porous titanium. Key Eng Mater. https://doi.org/10.4028/www.scientific.net/KEM.218-220.51
69. Li JP, Li SH, De Groot K, Layrolle P (2003) Improvement of porous titanium with thicker struts. Key Eng Mater. https://doi.org/10.4028/www.scientific.net/KEM.240-242.547
70. Kearns M, Blenkinsop P (1987) Manufacture of a novel porous metal. Met Mater 3(2):85–88
71. Dunand D, Teisen J (1998) Superplastic foaming of titanium and Ti-6Al-4V. MRS Online Proc Libr Arch. https://doi.org/10.1557/PROC-521-231521
72. Davis N, Teisen J, Schuh C, Dunand D (2001) Solid-state foaming of titanium by superplastic expansion of argon-filled pores. J Mater Res 16(5):1508–1519
73. Parthasarathy J, Starly B, Raman S, Christensen A (2010) Mechanical evaluation of porous titanium (Ti6Al4V) structures with electron beam melting (EBM). J Mech Behav Biomed Mater 3(3):249–259
74. Heinl P, Müller L, Körner C, Singer RF, Müller FA (2008) Cellular Ti–6Al–4V structures with interconnected macro porosity for bone implants fabricated by selective electron beam melting. Acta Biomater 4(5):1536–1544
75. Revathi A, Borrás AD, Muñoz AI, Richard C, Manivasagam G (2017) Degradation mechanisms and future challenges of titanium and its alloys for dental implant applications in oral environment. Mater Sci Eng C 76:1354–1368
76. Seah K, Thampuran R, Teoh S (1998) The influence of pore morphology on corrosion. Corros Sci 40(4–5):547–556
77. Fojt J, Joska L, Málek J (2013) Corrosion behaviour of porous Ti–39Nb alloy for biomedical applications. Corros Sci 71:78–83
78. Alves A, Sendão I, Ariza E, Toptan F, Ponthiaux P, Pinto A (2016) Corrosion behaviour of porous Ti intended for biomedical applications. J Porous Mater 23(5):1261–1268
79. Li Y-H, Rao G-B, Rong L-J, Li Y-Y, Ke W (2003) Effect of pores on corrosion characteristics of porous NiTi alloy in simulated body fluid. Mater Sci Eng A 363(1–2):356–359
80. Long M, Rack H (1998) Titanium alloys in total joint replacement—a materials science perspective. Biomaterials 19(18):1621–1639
81. Wu S, Liu X, Wu G, Yeung KW, Zheng D, Chung CY, Xu Z, Chu PK (2013) Wear mechanism and tribological characteristics of porous NiTi shape memory alloy for bone scaffold. J Biomed Mater Res A 101(9):2586–2601
82. Salahinejad E, Amini R, Marasi M, Hadianfard M (2010) Microstructure and wear behavior of a porous nanocrystalline nickel-free austenitic stainless steel developed by powder metallurgy. Mater Des 31(4):2259–2263
83. Liu Z, Ji F, Wang M, Zhu T (2017) Study on the tribological properties of porous titanium sliding against tungsten carbide YG6. Metals 7(1):28
84. Prabu SS, Prathiba S, Venkatesan N, Sharma A, Ahmed S, Shah YA (2014) Influence of Titanium on dry sliding wear behaviour of sintered P/M low alloy steel (Fe-CW). Proced Eng 97:2110–2118
85. Licausi M-P, Muñoz AI, Borrás VA (2013) Tribocorrosion mechanisms of Ti6Al4V biomedical alloys in artificial saliva with different pHs. J Phys D 46(40):404003
86. Mathew MT, Barão VA, Yuan JC-C, Assunção WG, Sukotjo C, Wimmer MA (2012) What is the role of lipopolysaccharide on the tribocorrosive behavior of titanium? J Mech Behav Biomed Mater 8:71–85

87. Doni Z, Alves A, Toptan F, Gomes J, Ramalho A, Buciumeanu M, Palaghian L, Silva F (2013) Dry sliding and tribocorrosion behaviour of hot pressed CoCrMo biomedical alloy as compared with the cast CoCrMo and Ti6Al4V alloys. Mater Des (1980–2015) 52:47–57
88. Licausi M-P, Muñoz AI, Borrás VA (2013) Influence of the fabrication process and fluoride content on the tribocorrosion behaviour of Ti6Al4V biomedical alloy in artificial saliva. J Mech Behav Biomed Mater 20:137–148
89. Dimah MK, Albeza FD, Borrás VA, Muñoz AI (2012) Study of the biotribocorrosion behaviour of titanium biomedical alloys in simulated body fluids by electrochemical techniques. Wear 294:409–418
90. Diomidis N, Mischler S, More N, Roy M (2012) Tribo-electrochemical characterization of metallic biomaterials for total joint replacement. Acta Biomater 8(2):852–859
91. Mathew MT, Abbey S, Hallab NJ, Hall DJ, Sukotjo C, Wimmer MA (2012) Influence of pH on the tribocorrosion behavior of CpTi in the oral environment: synergistic interactions of wear and corrosion. J Biomed Mater Res B 100(6):1662–1671
92. Souza JCM, Barbosa SL, Ariza E, Celis JP, Rocha LA (2012) Simultaneous degradation by corrosion and wear of titanium in artificial saliva containing fluorides. Wear 292:82–88
93. Cvijović-Alagić I, Cvijović Z, Mitrović S, Panić V, Rakin M (2011) Wear and corrosion behaviour of Ti–13Nb–13Zr and Ti–6Al–4V alloys in simulated physiological solution. Corros Sci 53(2):796–808
94. Majumdar P, Singh S, Chakraborty M (2011) The influence of heat treatment and role of boron on sliding wear behaviour of β-type Ti–35Nb–7.2 Zr–5.7 Ta alloy in dry condition and in simulated body fluids. J Mech Behav Biomed Mater 4(3):284–297
95. Majumdar P, Singh S, Chakraborty M (2010) Wear properties of Ti–13Zr–13Nb (wt.%) near β titanium alloy containing 0.5 wt.% boron in dry condition, Hank's solution and bovine serum. Mater Sci Eng C 30(7):1065–1075
96. Majumdar P, Singh S, Chakraborty M (2008) Wear response of heat-treated Ti–13Zr–13Nb alloy in dry condition and simulated body fluid. Wear 264(11–12):1015–1025
97. Komotori J, Hisamori N, Ohmori Y (2007) The corrosion/wear mechanisms of Ti–6Al–4V alloy for different scratching rates. Wear 263(1–6):412–418